

MEASUREMENT OF HIGH ENERGY DIRECT PHOTONS IN  $\psi$  DECAYS\*

G. S. Abrams, M. S. Alam, C. A. Blocker, A. M. Boyarski, M. Breidenbach, D. L. Burke, W. C. Carithers, W. Chinowsky, M. W. Coles, S. Cooper, W. E. Dieterle, J. B. Dillon, J. Dorenbosch, J. M. Dorfan, M. W. Eaton, G. J. Feldman, M. E. B. Franklin, G. Gidal, G. Goldhaber, G. Hanson, K. G. Hayes, T. Himel, D. G. Hitlin<sup>†</sup>, R. J. Hollebeek, W. R. Innes, J. A. Jaros, P. Jenni, A. D. Johnson, J. A. Kadyk, A. J. Lankford, R. R. Larsen, V. Lüth, R. E. Millikan, M. E. Nelson, C. Y. Pang, J. F. Patrick, M. L. Perl, B. Richter, A. Roussarie, D. L. Scharre, R. H. Schindler, R. F. Schwitters<sup>‡</sup>, J. L. Siegrist, J. Strait, H. Taureg, M. Tonutti<sup>§</sup>, G. H. Trilling, E. N. Vella, R. A. Vidal, I. Videau, J. M. Weiss, and H. Zaccane<sup>¶</sup>

Stanford Linear Accelerator Center  
Stanford University, Stanford, California 94305

and

Lawrence Berkeley Laboratory and Department of Physics  
University of California, Berkeley, California 94720

ABSTRACT

We have measured the inclusive  $\gamma$  and  $\pi^0$  momentum distributions at the  $\psi$ . Using these data and estimates of  $\eta$  production, we find that  $(4.1 \pm 0.8)\%$  of  $\psi$  decays contain a direct photon with energy greater than 60% of the beam energy. The expected momentum distribution for direct photons calculated to lowest-order in QCD is qualitatively different than that observed in the data.

(Submitted to Physical Review Letters)

---

\* Work supported primarily by the Department of Energy under contract numbers DE-AC03-76SF00515 and W-7405-ENG-48.

† Present address: California Institute of Technology, Pasadena, CA 91125.

‡ Present address: Harvard University, Cambridge, MA 02138.

§ Present address: Universität Bonn, D-53 Bonn, F. R. Germany.

¶ Present address: CEN-Saclay, F-91190 Gif-sur-Yvette, France.

First-order QCD calculations predict that a significant fraction of the hadronic decays of heavy quark-antiquark  $3S_1$  resonances (such as the  $\psi$ ) result in the production of direct  $\gamma$ 's (i.e.,  $\gamma$ 's not coming from secondary decays of  $\pi^0$ 's or  $\eta$ 's).<sup>1</sup> We have measured the inclusive  $\gamma$  and  $\pi^0$  momentum distributions at the  $\psi$ , and have made estimates of the  $\eta$  momentum distribution from the data. We observe  $\gamma$  production in excess of the expected contributions from  $\pi^0$  and  $\eta$  decay.

The data were collected with the Mark II magnetic detector at the SLAC  $e^+e^-$  storage ring facility SPEAR at energies near the peak of the  $\psi(3095)$  resonance. The detector has been described in detail elsewhere,<sup>2</sup> and only a brief description of the particle detection will be presented in this Letter.

Charged tracks are reconstructed from hits in the sixteen cylindrical drift chamber layers which provide solid angle coverage over 85% of  $4\pi$  sr. The trigger requires two or more charged tracks, one of which must be within the central region of the drift chamber which covers 67% of  $4\pi$  sr.

Photons are detected primarily in the eight lead-liquid argon (LA) shower counter modules which surround the solenoid, covering approximately 64% of  $4\pi$  sr. The rms energy resolution for detected photons is given approximately by  $\delta E/E = 0.12/E^{1/2}$  (E in GeV). The  $\gamma$  detection efficiency (including geometry) is approximately 30% at 0.2 GeV, 50% at 0.3 GeV, and 55% above 0.4 GeV.<sup>3</sup>

Neutral pions are reconstructed by combining pairs of  $\gamma$ 's each of which is required to have momentum greater than 150 MeV. Pairs with invariant mass between 0.075 and 0.200 GeV are considered to be  $\pi^0$

candidates. The  $\pi^0$  signal is extracted after subtraction of a background whose shape is a function of momentum. The background shape is obtained by combining real photons and "pseudo-photons" from the same event. Pseudo-photons are created in the analysis program by pretending that charged particles are  $\pi^0$ 's and allowing them to decay into pseudo-photons.<sup>4</sup> The background distribution is normalized to the data in the mass region between 0.3 and 1.0 GeV. Finally, a correction is made for tails of the  $\pi^0$  which fall outside the specified mass cuts. The  $\pi^0$  detection efficiency is 6% at 0.4 GeV, 18% at 0.6 GeV, and 30% at 1.0 GeV.

We have measured the inclusive  $\gamma$  and  $\pi^0$  momentum distributions at the  $\psi$  using a sample of 280,000 observed  $\geq 2$  prong hadron events. The trigger efficiency is measured by using a sample of events taken near the peak of the  $\psi'$ (3684). A sample of  $\psi$  events from the decay  $\psi' \rightarrow \psi \pi^+ \pi^-$  is obtained by requiring the missing mass from observed pairs of oppositely charged pions to be consistent with the mass of the  $\psi$  ( $m_\psi$ ).<sup>5</sup> This sample of  $\psi$  events is identified purely from the  $\pi^+$  and  $\pi^-$  and has no trigger bias arising from the  $\psi$  decay. As a function of  $\gamma$  or  $\pi^0$  momentum, the trigger efficiency is calculated as the fraction of events which satisfy the trigger requirement after elimination of the recoiling  $\pi^+$  and  $\pi^-$  from the event. The resulting trigger efficiency as a function of  $\gamma$  momentum  $p$  varies from 70% at  $x=0.1$  to approximately 40% near  $x=1.0$ , where  $x=2p/m_\psi$ . The trigger efficiency vs.  $\pi^0$  momentum varies from 70% at  $x=0.3$  to approximately 50% near  $x=1.0$ . From the average trigger efficiency (based on the entire event sample), the number of produced  $\psi$  events corresponding to the 280,000 observed hadron events is calculated to be 435,000.

Figure 1 shows the inclusive  $\gamma$  momentum distribution,  $(1/N_{\text{tot}})dN/dx$ , as a function of  $x$ , where  $N_{\text{tot}}$  is the total number of produced  $\psi$ 's. The error bars represent the statistical errors only. Overall systematic errors are approximately  $\pm 20\%$ , roughly half of which are independent of  $x$ . Corrections for detection and trigger efficiency have been made. Background due to the  $e^+e^-$  final state in which one of the electrons radiates a  $\gamma$  is eliminated. Radiation in the initial state is negligible. The inclusive  $\pi^0$  scaled momentum distribution is shown in Fig. 2. Systematic errors of  $\pm 30\%$ , much of which may be  $x$  dependent, are not shown in the figure.

From the measured  $\pi^0$  distribution, we have made predictions for the expected  $\gamma$  momentum distribution. In addition to the contribution from  $\pi^0$  decays, there is an additional contribution from  $\eta$  decays.<sup>6</sup> To determine the  $\eta$  population, we have made least-squares fits to the background-subtracted  $\gamma\gamma$  invariant-mass distributions in different momentum bins. The functional form used in the fits consists of a Gaussian, fixed at the  $\eta$  mass with width as determined by Monte Carlo calculation, over a linear background. We have measured the ratio  $R(p) = B(\psi \rightarrow \eta + X) \times B(\eta \rightarrow \gamma\gamma) / B(\psi \rightarrow \pi^0 + X)$  as a function of momentum. We find  $R(p)$  is less than 0.10 for all momentum bins except for  $p > 1.2$  GeV where we measure  $R = 0.16 \pm 0.06$ . From the measured value of  $R$  as a function of momentum, we estimate the contribution to  $\gamma$  production from  $\eta$ 's.

The  $\gamma$  momentum distribution predicted from the measured  $\pi^0$  and  $\eta$  momentum distributions is also shown in Fig. 1. The error bars include possible systematic errors ( $\pm 22\%$ ) which affect the measured and predicted  $\gamma$  distributions differently, but do not include correlated errors. We observe an excess of produced  $\gamma$ 's over the prediction for  $x \gtrsim 0.5$ .

Figure 3 shows the direct  $\gamma$  momentum distribution calculated by subtracting the expected distribution from  $\pi^0$ 's and  $\eta$ 's from the measured distribution. The error bars include the statistical error and the systematic error in the difference between the measured and predicted distributions. The errors become small at large  $x$  because the  $\pi^0$  contribution is small. For  $x < 0.4$ , the errors become too large to provide meaningful information, and only for  $x > 0.5$  can a clear excess be demonstrated. In addition to the displayed error bars, there is a  $\pm 17\%$  systematic error on the distribution due to uncertainties in the  $\gamma$  detection efficiency, the number of produced  $\psi$  events, the trigger efficiency, and the angular distribution of the direct  $\gamma$ 's as discussed below.

Figure 4 shows the distribution of observed photons with  $x > 0.6$  as a function of  $|\cos\theta|$ , where  $\theta$  is the polar angle of the  $\gamma$  with respect to the beam direction. The angular distribution has been fit to the form  $1 + \alpha_\gamma \cos^2\theta$  and gives  $\alpha_\gamma = 0.14 \pm 0.12$ . Approximately 25% of these events are background from  $\pi^0$  or  $\eta$  decays. Analysis of the angular distribution of photons from observed  $\pi^0$  decays shows this background to be consistent with an isotropic distribution. Correcting for this background gives  $\alpha_\gamma = 0.18 \pm 0.18$  for the direct  $\gamma$  contribution. An

overall correction of 3% is made to the data (which has been included in Fig. 3) to correct for the deviation of the observed angular distribution from isotropy. Integrating the direct  $\gamma$  momentum distribution from  $x=0.6$  to 1.0, we obtain an inclusive rate for direct photon production of  $(4.1 \pm 0.8)\%$ . This integrated cross section includes a correction (-6%) for feed-down from lower  $x$  due to the resolution of the LA.

As a check on possible systematic errors and trigger bias problems, this analysis has been repeated using two other independent methods. The first method makes use of photons which convert in the 0.06-radiation length of material preceding the drift chamber. The photons are reconstructed from measurement of the momenta of the resulting  $e^+$  and  $e^-$  in the drift chamber. Neutral pions are reconstructed from combinations of a converted  $\gamma$  and a  $\gamma$  observed in the LA. As essentially all  $\gamma$ 's which are detected through pair conversion satisfy the trigger requirement, no trigger bias is introduced in this method. The data are corrected for the  $\gamma$  and  $\pi^0$  detection efficiencies, which are calculated independently of those used in the LA. The second method makes use of the statistically independent sample of  $\psi$  events from the decay  $\psi' \rightarrow \psi \pi^+ \pi^-$ . As described above, this sample is free of trigger bias. The resulting  $\gamma$ ,  $\pi^0$ , and direct  $\gamma$  distributions measured with these alternative methods of analysis are consistent with the results of the analysis described previously.

First order QCD calculations<sup>1</sup> predict significant direct photon production at the  $\psi$ . The hadronic decay of the  $\psi$  must proceed via an intermediate state consisting of at least 3 color-octet gluons. One expects the dominant contribution to direct  $\gamma$  production to arise by

replacing one of the outgoing gluon lines by a  $\gamma$ . From lowest-order perturbation theory,

$$B_{\gamma} = \Gamma(\psi \rightarrow \gamma gg) / \Gamma(\psi \rightarrow ggg) = (\alpha/\alpha_s) C(e_Q/e)^2 ,$$

where  $C=36/5$  is a color SU(3) factor,  $e_Q$  is the charge of the charmed quark, and  $\alpha_s$  is the color fine-structure constant. For  $\alpha_s=0.18$ ,<sup>7</sup> one calculates  $B_{\gamma}=13\%$  for all  $x$ . Equating the direct decay of the  $\psi$  into hadrons with the 3-gluon decay, and correcting for second-order electromagnetic decays, the lowest order QCD prediction for the branching ratio for direct  $\gamma$  decays from the  $\psi$  is 8%. The  $\gamma$  momentum spectrum is predicted to be roughly proportional to  $x$  and peak near  $x=1.0$ . The lowest-order QCD prediction (convoluted with the  $\gamma$  energy resolution) is shown compared to the data in Fig. 3. Although the total rate of direct  $\gamma$  production approximately agrees with theoretical expectations (one expects 5% for  $x > 0.6$ ), and the mean value of the coefficient of the  $\cos^2\theta$  term in the angular distribution agrees with theory (one expects  $\alpha_{\gamma} \approx 0.3$  for  $x > 0.6$ ), the shape of the observed distribution is inconsistent with the prediction. However, it is expected that the observed distribution should be softer than the leading-order prediction since radiative effects and the mass of the final-state hadrons are not considered, but no calculation has been made. One calculation for the decay width of a heavy quark-antiquark bound state indicates that higher-order effects are of the same magnitude as lower-order terms,<sup>8</sup> thus making it difficult to provide accurate theoretical predictions.

In conclusion, we have measured direct photon production at the  $\psi$  at large  $x$ . We find that  $(4.1 \pm 0.8)\%$  of  $\psi$  decays produce a direct photon with  $x > 0.6$ .<sup>9</sup> The observed rate is consistent with lowest-order QCD predictions, but the observed distribution is softer.

This work was supported primarily by the Department of Energy under contract numbers DE-AC03-76SF00515 and W-7405-ENG-48.



REFERENCES

1. T. Appelquist et al., Phys. Rev. Lett. 34, 365 (1975); M. Chanowitz, Phys. Rev. D12, 918 (1975); L. Okun and M. Voloshin, ITEP-95-1976 (unpublished); S. J. Brodsky et al., Phys. Lett. 73B, 203 (1978); K. Koller and T. Walsh, Nucl. Phys. B140, 449 (1978).
2. G. S. Abrams et al., Phys. Rev. Lett. 43, 477 (1979); G. S. Abrams et al., Phys. Rev. Lett. 43, 481 (1979).
3. These efficiencies were obtained by Monte Carlo simulation of the electromagnetic shower development [see R. L. Ford and W. R. Nelson, SLAC Report No. 210, 1978 (unpublished)] in the Mark II detector assuming isotropic production of  $\gamma$ 's. These efficiencies agree with measured efficiencies obtained by studying the decays  $\psi \rightarrow \pi^+ \pi^- \pi^0$  and  $\psi \rightarrow \pi^+ \pi^- \pi^+ \pi^- \pi^0$ .
4. It is assumed that the charged particle and  $\pi^0$  momentum distributions are similar. Resolution and efficiency effects are included in the generation of pseudo-photons in order to simulate the observed photon spectrum.
5. The background from accidental combinations falling in the  $\psi$  mass region is estimated using events in bands on either side of the peak and subtracted.
6. The contribution from radiative decays of other secondary hadrons is estimated to be negligible compared to the overall uncertainty in the  $\pi^0$  contribution. For instance,  $\eta'$  production equal to  $\eta$  production would change the estimated direct  $\gamma$  rate for  $x > 0.6$  by less than 3%.

7. This value of  $\alpha_s$  is calculated from the ratio of the leptonic to the hadronic width of the  $\psi$  [see T. Appelquist and H. D. Politzer, Phys. Rev. Lett. 34, 43 (1975)]. The predicted direct  $\gamma$  contribution is included as part of the total width of the  $\psi$  used in the calculation.
8. R. Barbieri et al., Nucl. Phys. B154, 535 (1979).
9. Another experiment [M. T. Ronan et al., LBL-9256 (1979)] finds evidence of production of direct  $\gamma$ 's consistent in magnitude with this experiment.

FIGURE CAPTIONS

1. Solid points show the inclusive  $\gamma$  momentum distribution  $(1/N_{\text{tot}})dN/dx$ . Open points show the expected  $\gamma$  momentum distribution based on measurements of  $\pi^0$  and  $\eta$  production. The error bars on the measured  $\gamma$  distribution reflect only the statistical errors, whereas the error bars on the expected distribution include a  $\pm 20\%$  systematic error.
2. Inclusive  $\pi^0$  momentum distribution  $(1/N_{\text{tot}})dN/dx$ , where  $x = 2p/m_\psi$ . Systematic errors of  $\pm 30\%$  are not shown in the figure.
3. Direct  $\gamma$  momentum distribution. Curve is the leading-order QCD prediction convoluted with the energy resolution.
4. Angular distribution of observed photons with  $x > 0.6$  as a function of  $|\cos\theta|$ . Curve represents the best fit to the form  $1 + \alpha_\gamma \cos^2\theta$ .

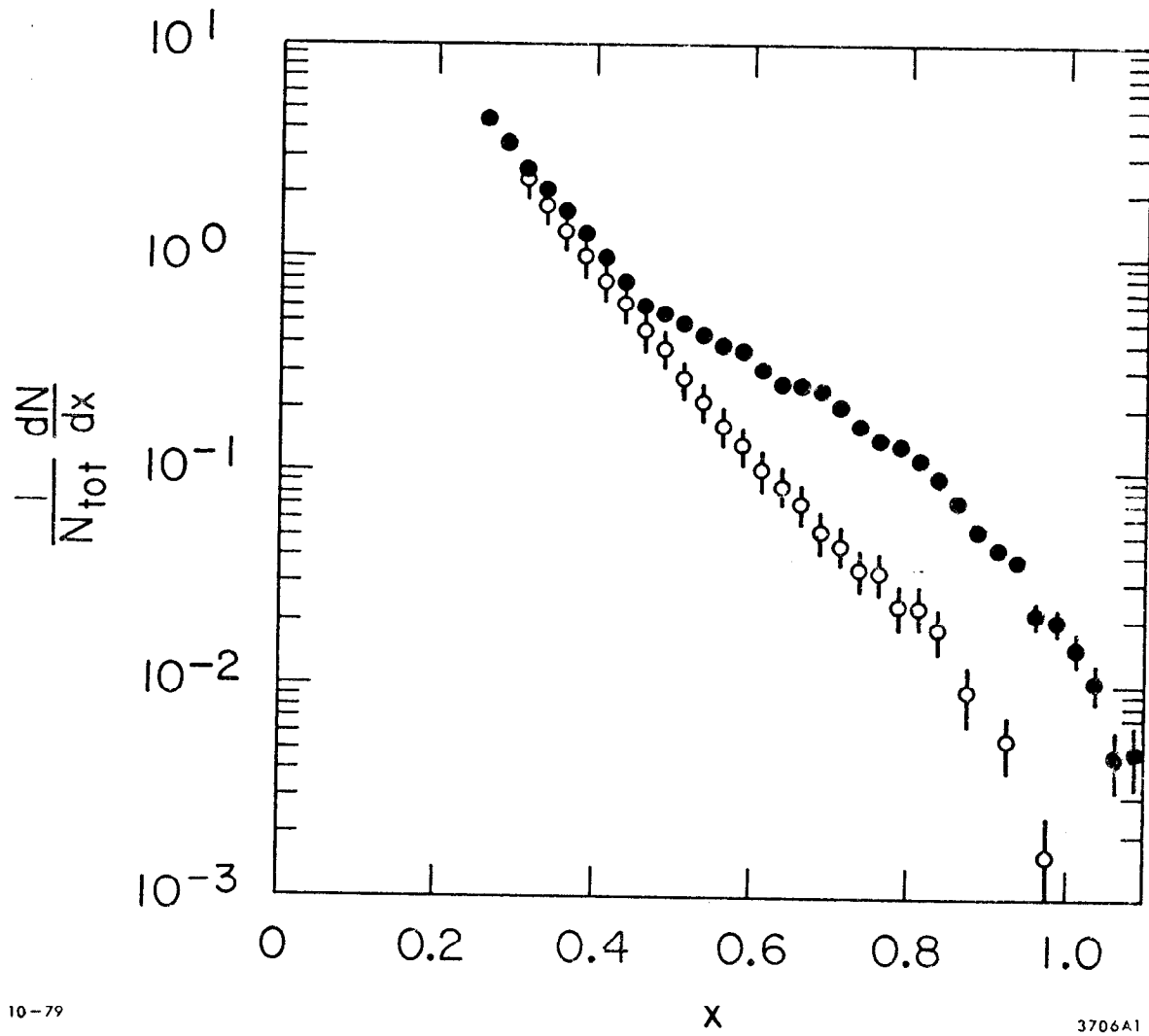


Fig. 1

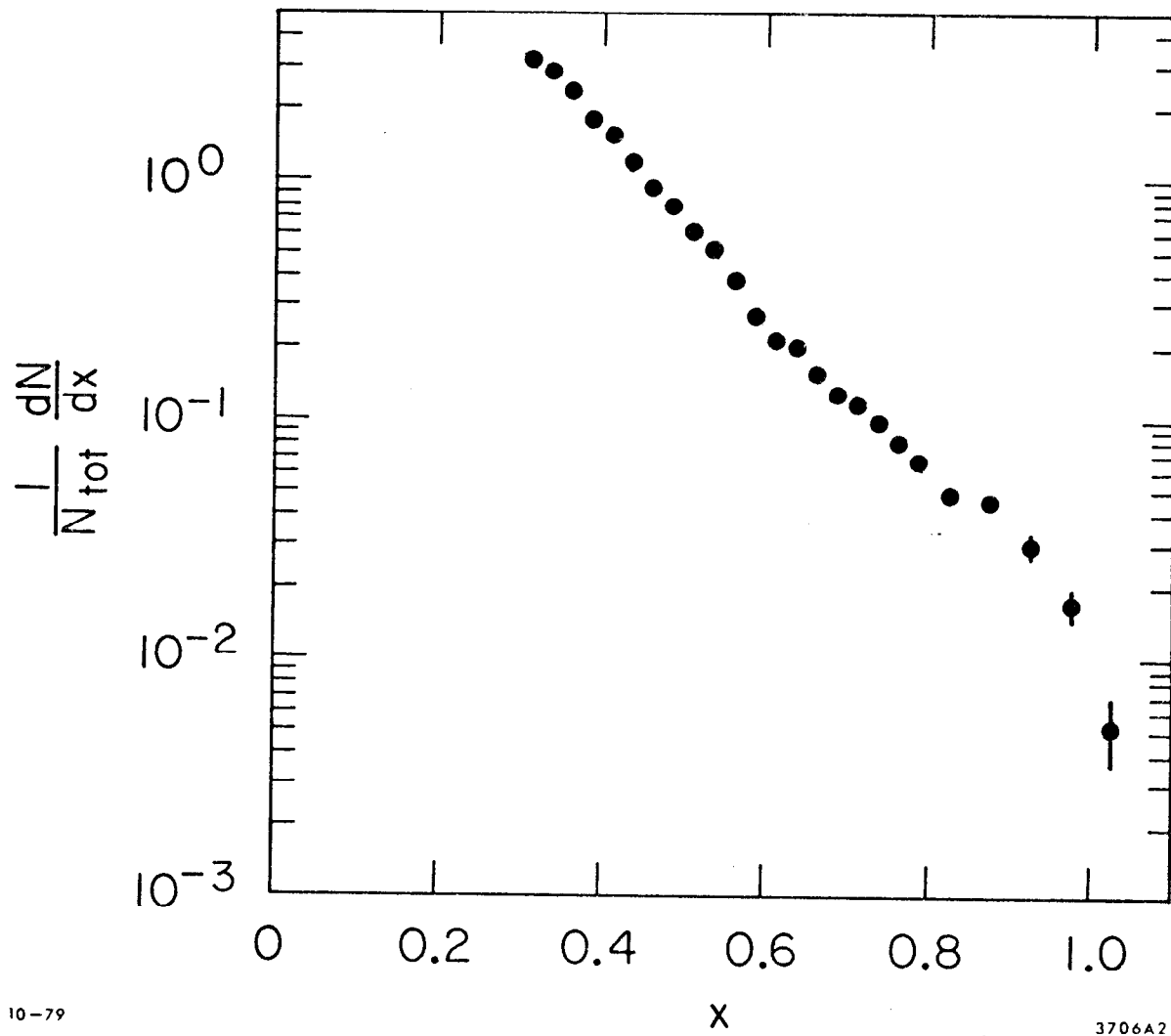


Fig. 2

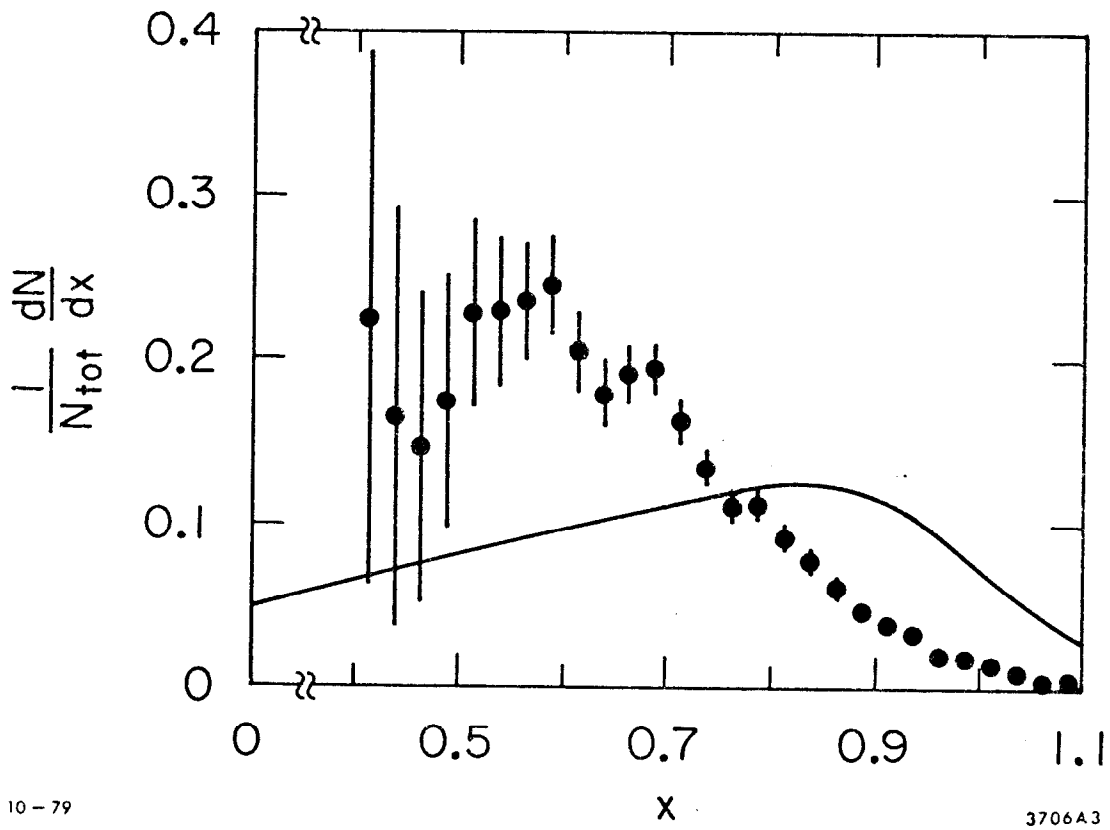


Fig. 3

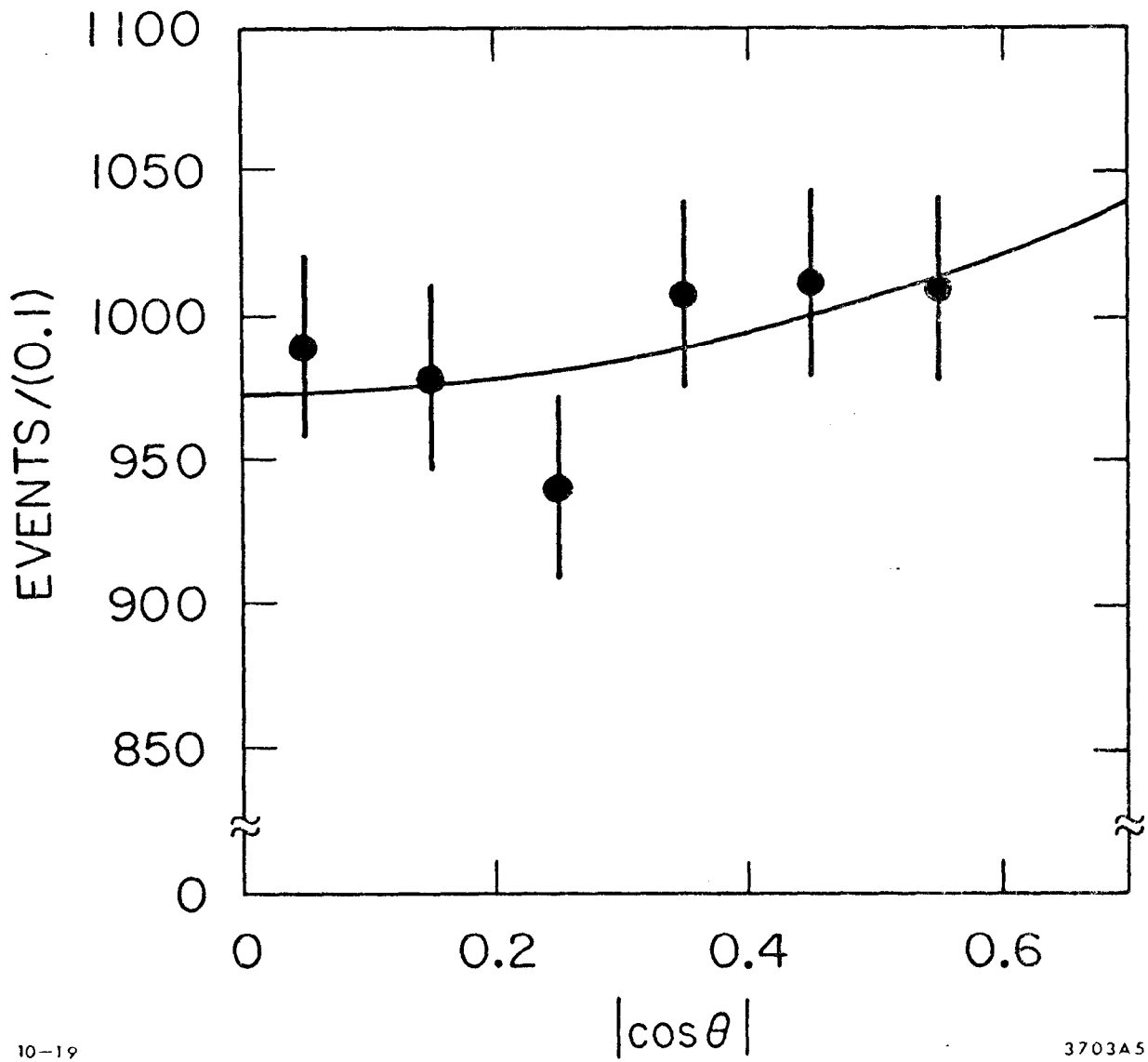


Fig. 4